

---

# Transferring Textual Knowledge for Visual Recognition

---

Wenhao Wu<sup>1,2</sup>    Zhun Sun<sup>2</sup>    Wanli Ouyang<sup>1,3</sup>

<sup>1</sup>The University of Sydney    <sup>2</sup>Baidu Inc.    <sup>3</sup>Shanghai AI Laboratory  
whwu.ucas@gmail.com

## Abstract

Transferring knowledge from task-agnostic pre-trained deep models for downstream tasks is an important topic in computer vision research. Along with the growth of computational capacity, we now have open-source Vision-Language pre-trained models in large scales of the model architecture and amount of data. In this study, we focus on transferring knowledge for vision classification tasks. Conventional methods randomly initialize the linear classifier head for vision classification, but they leave the usage of the text encoder for downstream visual recognition tasks undiscovered. In this paper, we revise the role of the linear classifier and replace the classifier with the embedded language representations of the object categories. These language representations are initialized from the text encoder of the vision-language pre-trained model to further utilize its well-pretrained language model parameters. The empirical study shows that our method improves both the performance and the training speed of video classification, with a negligible change in the model. In particular, our paradigm achieves the state-of-the-art accuracy of 87.8% on Kinetics-400. Code: <https://github.com/whwu95/Text4Vis>.

## 1 Introduction

Pre-training a task-agnostic model using large-scale general datasets and then transferring its learning feature representations to downstream tasks is a paradigm in many computer vision applications [1, 2]. While in the last decade, the convolutional-based models that are optimized on the ImageNet [3] (more precisely, ILSVRC-2012) dataset with a supervised style dominated this field. Owing to the dramatically increasing computational capacity, now we can train models that have several magnitude more model parameters and FLOPs on significantly larger datasets in either supervised [4, 2, 5], weakly-supervised [1, 6] or self-supervised [7, 8] style. Recently, contrastive learning-based vision-language pre-training [1] manifest their superior capabilities in improving down-streaming tasks performance such as classification [1], captioning [9], image generation [10, 11], to name a few. These models are powerful for two reasons: i) the employed large-scale weakly-related datasets provide rich semantics and diverse representations of concepts; ii) the representation vectors of images and texts are roughly aligned in the semantic embedding space. However, the most common approach to using these models is fine-tuning the visual encoder on specific tasks. Although the rich semantics and diverse representations of concepts benefit the downstream tasks, the usage of the textual encoder is still left undiscovered.

In this study, we aim to improve the transferability of such vision-language pre-training models for downstream classification tasks, with the help of their textual encoders. Our motivation comes from the semantic similarity among the ground-truth labels. To demonstrate this, we employ the kinetics video recognition dataset [12] for the analysis. We extract the embedded textual vectors of class labels using the textual encoder released by CLIP [1]. We then calculate the correlation between the embedded textual vectors. The plot is shown on the left of Figure 1. Not surprisingly, the extracted

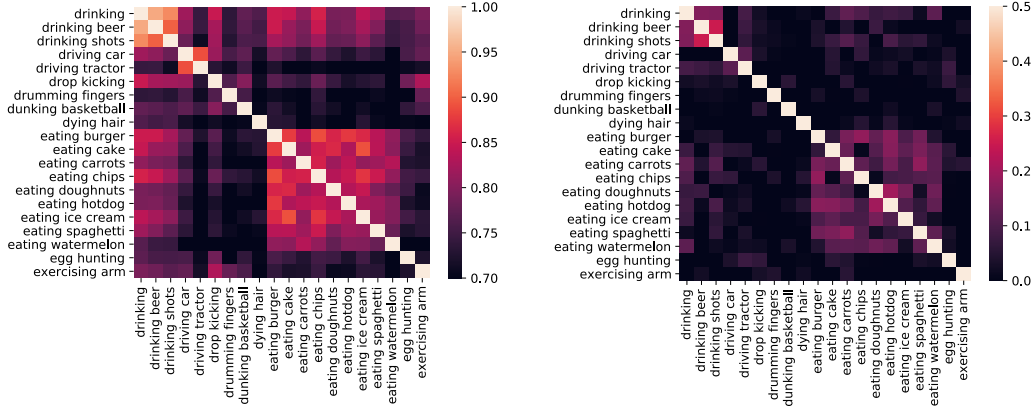


Figure 1: Inter-class correlation maps of “embeddings of class labels” for 20 categories on Kinetics-400. **Left:** The extracted textual vectors of class labels, **Right:** The “embeddings” from learned classifier. The color thresholds are adjusted for better understandability. Please zoom in for best view.

textual vectors of class labels exhibit certain inter-class correlations, since part of them include the same verbs in their labels, such as *playing <something>*. Meanwhile, the labels with different verbs show a negligible inter-class correlation, such as *drinking* and *driving*. Next, we examine the final projection head of a vanilla visual recognition framework. We conduct the visual-only fine-tuning progress with the visual encoder that is also released by CLIP [1]. The detailed configurations are provided in Section 4.3. The projection head is a matrix of  $d \times c$  to compute the pre-softmax values (or logits) from the  $d$ -dimensional feature vectors for the  $c$  classes. Non-rigorously, we can consider the  $d$ -dimensional row vectors as the embeddings of the class labels, allowing us to explore the inter-class correlation between these learned “embeddings”, as shown on the right side of Figure 1. Interestingly, these learned “embeddings” also reveal certain correlations after the training progress, despite being initialized randomly and optimized without knowing any textual information<sup>1</sup>.

Therefore, we suppose that the semantic information contained in the samples (images and videos) does correlate with inter-classes. Following this motivation, we replace the projection matrix with several variants: i) A projection matrix whose row vectors are randomly sampled (trivial correlation); ii) A projection matrix whose row vectors are orthogonal to each other (non-correlated). Then we replace the projection matrix with fixed embedded textual vectors that provide the “proper” correlation. In the empirical studies, we find that the textual knowledge significantly improves the transferability of pre-trained models, regarding both the classification accuracy and the convergence speed. Our main contributions are summarized as follows:

- We build a new recognition paradigm to improve the transferability using knowledge from the textual encoder of the well-pretrained vision-language model.
- We conduct extensive experiments on popular video and image datasets (*i.e.*, Kinetics-400 [12], UCF-101 [13], HMDB-51 [14] and ImageNet [3]) to demonstrate the transferability of our solution in many types of transfer learning, *i.e.*, image/video recognition, zero-shot recognition, few-shot recognition. Our approach democratizes the training on large-scale video/image datasets and achieves state-of-the-art performance on video recognition tasks, *e.g.*, 87.3% top-1 accuracy on Kinetics-400.

## 2 Methodology

**Denotations.** In the rest of the paper, we use bold letters to denote Vector, and capital italic letters to denote Tensor or Matrix. For instance, we employ  $\mathbf{z} \in \mathbb{R}^d$  to denote the feature vector extracted from a pre-trained model of dimension  $d$ , we employ  $W \in \mathbb{R}^{d \times c}$  to denote the projection matrix for the  $c$ -class linear classifier. Without ambiguity, we also use capital italic letters to denote the

<sup>1</sup>That is, optimized with cross-entropy loss with one-hot labels

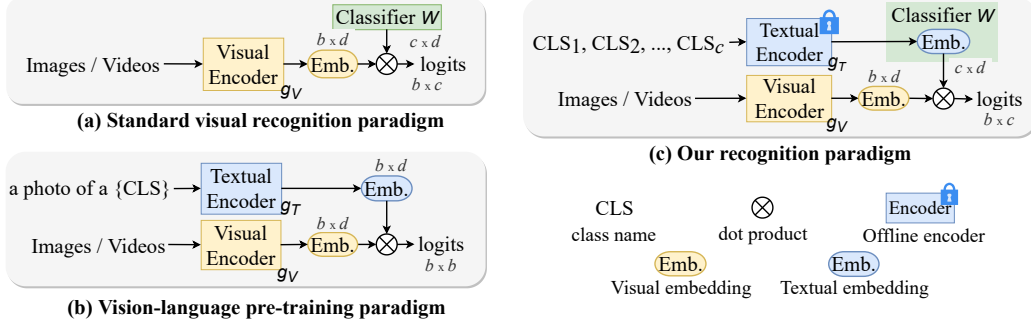


Figure 2: Illustration of (a) standard visual recognition paradigm, (b) vision-language pretraining paradigm, and (c) our proposed recognition paradigm.

modality in subscripts, especially we employ  $V$  and  $T$  to denote the *Visual* modality and *Textual* modality, respectively. We further employ lowercase italic letters to denote functions or neural networks. For instance, we employ  $g_V(\cdot, \Theta_V)$  and  $g_T(\cdot, \Theta_T)$  to denote the visual encoder and textual encoder, respectively. Additionally, we employ calligraphic letters, *e.g.*,  $\mathcal{D}$ , to denote sets of elements.

## 2.1 Revisiting of the standard paradigm and the vision-language pre-training

**Standard visual feature transferring paradigm.** We start with the most ordinary scenario, where a visual feature encoder model  $g_V$  is optimized using a large-scale dataset  $\mathcal{D}$  that contains visual samples with or without ground-truth labels. On our labeled downstream dataset  $\hat{\mathcal{D}} = \{(\mathbf{x}_1, \mathbf{y}_1), (\mathbf{x}_2, \mathbf{y}_2), \dots\}$ , our empirical learning target can be written as

$$g_V^*, W^* = \operatorname{argmin}_{\Theta_V, W} \mathbb{E}_{\mathbf{x}, \mathbf{y} \sim \hat{\mathcal{D}}} [H(\mathbf{y} | \sigma(W \cdot g_V(\mathbf{x})))], \quad (1)$$

where  $H(\hat{p} | p)$  stands for the **CrossEntropy** between the predicted distribution  $p$  and the ground-truth distribution  $\hat{p}$ ,  $\sigma$  denotes the **softmax** operation,  $W \in \mathbb{R}^{c \times d}$  denotes the linear projection matrix for classification. The formulation in Eq. 1 is a standard visual feature transferring paradigm, where the visual encoder  $g_V$  and the projection matrix (classifier)  $W$  are learned simultaneously.

**Vision-language pre-training in CLIP.** As shown in Figure 2(b), we then review the contrastive pre-training paradigm of the vision-language models in [1]. Given a weakly related image-text pair dataset  $\mathcal{D} = \{(\mathbf{x}_{V,1}, \mathbf{x}_{T,1}), (\mathbf{x}_{V,2}, \mathbf{x}_{T,2}), \dots\}$ . With slight abuse of the notations, we employ the  $\mathbf{x}_V, \mathbf{x}_T$  to denote a mini-batch of size  $b$ , then we minimize the following target,

$$g_V^*, g_T^* = \operatorname{argmin}_{\Theta_V, \Theta_T} \mathbb{E}_{\mathbf{x}_V, \mathbf{x}_T \sim \mathcal{D}} [H(\mathcal{Q} | \sigma(g_V(\mathbf{x}_V)^T \cdot g_T(\mathbf{x}_T)))], \quad (2)$$

where  $\mathcal{Q}$  is the set that contains  $b$  one-hot labels of size  $c$ , with their  $1, 2, \dots, b$ -th element being 1 ( $b < c$ , denoting the positive image-text pairs). Here we clarify that, the formulation in Eq. 2 is not the rigorous form of the Noise-Contrastive Estimation (NCE) loss proposed in [15, 16]. Instead, we employ the cross entropy version implementation in [1, 17]. This implementation depicts a connection between the standard feature transferring paradigm and ours. In which, the  $g_T(\mathbf{x}_T)$  can be considered as the projection matrix that map the visual feature  $g_V(\mathbf{x}_V)$  to the given label set  $\mathcal{Q}$ .

## 2.2 Our proposed paradigm

As discussed in Section 1, we replace the learnable randomly initialized linear projection matrix  $W$  with pre-defined matrix  $\tilde{W}$ . Similarly, the training target can be written as

$$g_V^* = \operatorname{argmin}_{\Theta_V} \mathbb{E}_{\mathbf{x}, \mathbf{y} \sim \hat{\mathcal{D}}} [H(\mathbf{y} | \sigma(\tilde{W} \cdot g_V(\mathbf{x})))]. \quad (3)$$

Note that  $\tilde{W}$  is not in the optimization targets, since we freeze it from updating during the fine-tuning on the downstream tasks. We do this for two reasons: Firstly, it could preserve the textual knowledge from being disturbed by the randomness brought by the mini-batch. For instance, when some classes

are missing, their embedded feature vector might be broken by the other classes; Secondly, we want to provide a fair comparison between different initializations of  $\tilde{W}$  (The unfrozen results are given in the Appendix §A.4). Now we consider how to initialize  $\tilde{W}$ . To examine how the correlation between the semantic information contained in the samples helps, we investigate the following four types of initialization, where the forth is our proposed initialization.

**Randomized matrix** For the most simple randomized matrix case, we set each row of the  $\tilde{W}$  with a random Gaussian vector of zero mean and standard deviation, that is

$$\tilde{W} \sim \mathcal{N}(\mathbf{0}, I_d), \quad (4)$$

where  $I_d$  denotes the identity matrix of dimension  $d \times d$ . Arithmetically, a trivial “correlation” would appear between the row of the  $\tilde{W}$ , since the sampling size is significantly small to be biased. Evidently, the trivial “correlation” cannot indicate the real correspondence between the classes due to its stochasticity. Therefore we expect the model to have inferior performance since it needs to avoid these incorrect correlations when learning the visual feature representation.

**Randomized Orthogonal matrix** We follow the approach of the randomized matrix. We then remove the correlation by ensuring the row vectors are orthogonal. This is achieved by QR decomposition. Concretely, since  $d > c$ , we first generate a random matrix of size  $d \times d$  and select the first  $c$  rows as our projection matrix. Formally, we have,

$$\tilde{W}_j \sim \text{QR}(U)_j, j = 1, 2, \dots, c, \quad U_i \sim \mathcal{N}(\mathbf{0}, I_d), i = 1, 2, \dots, d, \quad (5)$$

where  $U$  is the intermediate randomized matrix,  $\text{QR}(U)$  is the row orthogonal matrix obtained through the QR decomposition. Similar to the randomized matrix, we also expect this initialization to have inferior performance. Given the fact that the one-hot label vectors are also orthogonal to each other, it will not be helpful to project the visual feature vectors with an orthogonal matrix, which increases the difficulty of learning meaningful visual features.

**Linear discriminant projection** We consider another way of initializing the projection matrix. We employ the multi-class Fisher’s linear discriminant analysis (LDA) to learn a linear classifier, then employ the weight matrix of the classifier as our initialization of the projection matrix. The LDA is optimized using the visual embeddings from the pre-trained model of samples in the train split. Then we compute the projection matrix following previous work [18]. Intuitively, the LDA first projects the feature vectors into a lower dimension space that maximizes the inter-class covariance and then estimates the likelihood of a sample to the class distributions. We, therefore, term this as the maximal correlation initialization. As an essential classifier, this type of initialization delivers reasonable performance, but it is largely dependent on the data employed to compute the projection matrix. When the data is limited, the estimated correlation will be biased. On the other hand, in our proposed paradigm, the pretrained textual encoder provides unbiased correlations for fine-tuning.

**Textual embedding vectors** We finally describe our proposed feature transferring paradigm. Briefly, the projection weight  $\tilde{W}$  is composed of the embedded textual feature vectors of the labels. Given a set of tokenized class labels  $\mathcal{L} = \{l_1, l_2, \dots, l_c\}$ , we have

$$\tilde{W}_i \sim g_T(l_i), i = 1, 2, \dots, c, \quad (6)$$

where  $\tilde{W}_i$  the  $i$ -th row vector in matrix  $\tilde{W}$ . And  $\tilde{W}_i$  is initialized using the textual encoder output of the textual label of the  $i$ -th class. In the experimental analysis, we investigate two types of textual feature encoders: i) The encoder that is trained with a visual encoder in the contrastive style; ii) The encoder that is trained solely using only textual samples on tasks such as masked language modeling.

### 3 Related Works

**Visual Recognition.** Convolutional networks have long been the standard for backbone architectures in image recognition [19, 20, 21, 22, 23, 24] and video recognition [25, 26, 27, 28, 29, 30, 31]. Inspired by the Transformer [32] scaling successes in Natural Language Processing, Vision Transformer (ViT) [33] applies a standard Transformer directly to images, which delivers impressive performance on image recognition. Since then, ViT [33] has led a new trend in image recognition backbone architectures, shifting from CNNs to Transformers. To improve performance, follow-up studies (*e.g.*, DeiT [34], Swin [35]) have been developed. Also, many works has begun to adopt transformers in video recognition, such as TimeSFormer [36], ViViT [37], VideoSwin [38], and MViT [39].

**Vision-language Pre-training.** Recently, CLIP [1] provides good practice in learning the coordinated vision-language pretraining models using the image-text InfoNCE contrastive loss [40]. Based on CLIP, several variants [41, 42, 43, 44, 45] have been proposed by combining more types of learning tasks such as image-text matching and masked image/language modeling. These contrastively learned models have two deserved properties for downstream tasks: the abundant visual feature representations and the aligned textual feature representations. Yet another study [46] merged the downstream classification task into the pretraining progress, which demonstrates a decent improvement of accuracy over the standard cross-entropy loss. Recently, many video-text retrieval methods [47, 48, 49, 50, 51, 52, 49, 53] have benefited from vision-language pre-training as well. Moreover, a few recent works [54, 55] transfer the CLIP [1] pre-trained image-text matching model to the downstream video-text matching framework for video recognition with contrastive loss. Specifically, ActionClip [54] extends the CLIP [1] to train a downstream video-text matching model and then perform video recognition indirectly using the similarity between learned video and text encoders during inference. [55] focus on efficient prompting and learning the continuous prompt template as text input for video recognition. Instead of these matching-based approaches, we aim to propose a new recognition paradigm that directly transfers textual knowledge for visual recognition. Our approach can balance performance and efficiency, and experiments demonstrate that our approach can reduce computational power requirements while democratizing training on large-scale video/image datasets (see Table 9 and 12 for more information).

## 4 Experiments: Video Recognition

### 4.1 Setups

To evaluate our method for video recognition, we conduct experiments on three widely used benchmarks, *i.e.*, Kinetics-400 [12], UCF-101 [13] and HMDB-51 [14]. See Appendix §A.1 for more details.

**Training & Inference.** We utilize ResNet [20] and ViT [33] as the visual encoders since they are the representative backbones of CNN and vision transformer, respectively. We employ the pre-trained visual and textual encoder released by CLIP [1] in most experiments for simplicity. Given a video, we first uniformly sampled  $T$  (*e.g.*, 8, 16, 32) frames over the entire video. Then image patches with the resolution of  $224 \times 224$  are randomly resized cropped from the sampled frames to form the input. We use RandAugment for the data augmentation. The model is optimized using AdamW with momentum set to 0.9. We use an initial learning rate of  $5e^{-6}$ , a cosine learning rate schedule with a 5-epoch linear warmup and a batch size of 256 for experiments on all datasets. For fast training, we set the total training epoch to 30 unless specified otherwise.

To trade off accuracy and speed, we consider two evaluation protocols. (1) *Single View*: We use only 1 clip per video and the center  $224 \times 224$  crop for efficient evaluation, (*e.g.*, as in Section 4.3). (2) *Multiple Views*: This is a widely used setting in previous works [56, 27, 57] to sample multiple clips per video (*e.g.*, 10 clips) with several spatial crops (*e.g.*, 3 crops) in order to get higher accuracy. For comparison with SOTAs, we use four clips with three  $224 \times 224$  crops (“4×3 Views”) in Table 1.

### 4.2 Main Results.

**Comparison to state-of-the-art.** In Table 1, on Kinetics-400, we compare to state-of-the-arts that are pre-trained on large-scale datasets such as ImageNet-21K [3], IG-65M [63], JFT-300M [2], FLD-900M [44] and JFT-3B [5]. The suffix represents the magnitude of the dataset, *e.g.*, JFT-3B consists of nearly 3 billion annotated images. We include the details of these web-scale datasets in Appendix §B.1. To the best of our knowledge, up to now, none of the three largest datasets (*i.e.*, JFT-300M, FLD-900M, JFT-3B) are open-sourced and also do not provide pre-trained models. Thus, we use the CLIP [1] checkpoints, which are publicly available<sup>2</sup> and have been trained on 400 million web image-text pairs (namely WIT-400M). Observe that we achieve state-of-the-art results. Specifically, our model outperforms all JFT300M-pretrained methods in terms of Top-1 and Top-5 accuracy. We achieve 87.3%, which improves even further by 0.8% over Florence [44], although their model and data scale are both  $2 \times$  larger. Besides, our model is even better than JFT3B-pretrained

<sup>2</sup><https://github.com/openai/CLIP/blob/main/clip/clip.py>

Table 1: Comparison to SOTAs on Kinetics-400. “Views” indicates # temporal clip  $\times$  # spatial crop. The magnitudes are Giga ( $10^9$ ) and Mega ( $10^6$ ) for FLOPs and Param. “IN” denotes ImageNet.

Method	Input	Pre-train	Top-1	Top-5	FLOPs $\times$ Views	Param
NL I3D-101 [27]	$128\times 224^2$	IN-1K	77.7	93.3	$359\times 10\times 3$	61.8
MVFNNet $_{E_n}$ [57]	$24\times 224^2$	IN-1K	79.1	93.8	$188\times 10\times 3$	-
SlowFast NL101 [56]	$16\times 224^2$	Scratch	79.8	93.9	$234\times 10\times 3$	59.9
X3D-XXL [58]	$16\times 440^2$	Scratch	80.4	94.6	$144\times 10\times 3$	20.3
MViT-B, $64\times 3$ [39]	$64\times 224^2$	Scratch	81.2	95.1	$455\times 3\times 3$	36.6
<i>Methods with large-scale pre-training</i>						
TimeSformer-L [36]	$96\times 224^2$	IN-21K	80.7	94.7	$2380\times 1\times 3$	121.4
ViViT-L/16 $\times 2$ [37]	$32\times 320^2$	IN-21K	81.3	94.7	$3992\times 4\times 3$	310.8
VideoSwin-L [38]	$32\times 384^2$	IN-21K	84.9	96.7	$2107\times 10\times 5$	200.0
ip-CSN-152 [59]	$32\times 224^2$	IG-65M	82.5	95.3	$109\times 10\times 3$	32.8
ViViT-L/16 $\times 2$ [37]	$32\times 320^2$	JFT-300M	83.5	95.5	$3992\times 4\times 3$	310.8
ViViT-H/16 $\times 2$ [37]	$32\times 224^2$	JFT-300M	84.8	95.8	$8316\times 4\times 3$	647.5
TokLearner-L/10 [60]	$32\times 224^2$	JFT-300M	85.4	96.3	$4076\times 4\times 3$	450
MTV-H [61]	$32\times 224^2$	JFT-300M	85.8	96.6	$3706\times 4\times 3$	-
CoVeR [62]	$16\times 448^2$	JFT-300M	86.3	-	$-\times 1\times 3$	-
Florence [44]	$32\times 384^2$	FLD-900M	86.5	97.3	$-\times 4\times 3$	647
CoVeR [62]	$16\times 448^2$	JFT-3B	87.2	-	$-\times 1\times 3$	-
Ours ViT-L/14	$32\times 224^2$	WIT-400M	87.1	97.4	$1662\times 4\times 3$	230.7
Ours ViT-L/14	$32\times 336^2$	WIT-400M	<b>87.8</b>	<b>97.6</b>	$3829\times 1\times 3$	230.7

CoVeR [62], and their data scale is  $7.5\times$  larger. See Appendix §A.2 for more results on UCF-101 and HMDB-51 datasets.

**Few-shot video recognition.** Video recognition using only a few samples is known as few-shot video recognition. We study a more challenging  $K$ -shot  $C$ -way situation instead of the conventional 5-shot 5-way configuration. We scale the task up to categorize **all** categories in the dataset with just  $K$  samples per category for training. The upper bound of this situation is denoted by the term “All-shot”. Table 2 reports the top-1 accuracy for the three datasets. In this extreme scenario of few data, we use 200 epochs to train models with ViT-B/16 for few-shot video recognition. For temporal modeling, we use TAP. We can observe that our method provides amazing transferability on diverse domain data in these extreme data-poor circumstances.

Table 2: Few-shot video recognition on three popular datasets under  $K$ -shot  $C$ -way setting.

K-shot	K400	UCF101	HMDB51
1	63.16	88.77	65.17
3	67.50	92.78	69.99
5	69.89	93.87	71.03
All	80.13	95.24	73.18

Table 3: Zero-shot video recognition under intra-dataset and cross-dataset settings.  $\{A\}\rightarrow\{B\}$  indicates we train the model on dataset A then perform zero-shot recognition on dataset B.

	K300 $\rightarrow$ K100	K400 $\rightarrow$ UCF
Ours w/o train	63.35	63.01
Ours w/ train	<b>66.38</b>	<b>74.67</b>

**Zero-shot video recognition.** We conduct experiments on two open-set settings: 1) Intra-dataset: The Kinetics-400 was divided into two parts: 300 categories (K300) for training and 100 categories (K100) for zero-shot recognition. 2) Cross-dataset: We train our models on K400 and then evaluate them on UCF101. To avoid catastrophic forgetting [64], here we train our models with few epochs. As shown in Table 3, unlike the traditional recognition paradigm, ours can achieve zero-shot recognition for unseen categories by replacing the offline classifiers. Appropriately tweaking the pre-trained model slightly can boost performance even further.

### 4.3 Ablations on Kinetics.

In this section, we conduct extensive ablation experiments to demonstrate our method with the instantiation. Models in this section use 8-frame input, ViT-B/16 as the visual backbone, 30 epochs for training and a single view for testing on Kinetics-400, unless specified otherwise.

**Comparison with vision-only framework.** Figure 2(a) illustrates the standard visual recognition framework. As a comparison with our method, we train the unimodality video model, which consists of the same visual encoder and a learnable classifier with random initialization. To produce video embedding, we just apply temporal average pooling (TAP) to frame embeddings. As presented in Figure 3, our method surpasses *Vision-Only* baselines across multiple label fractions on Kinetics-400. Especially when just only 10% labeled data is available for training, demonstrating that the advantage of our paradigm is more profound when the labeled data is limited. Also, when training with full data, our *Vision-Text* method leads to an additional 5% improvement with the same training recipe. Figure 4 further demonstrates our paradigm significantly improves convergence speed.

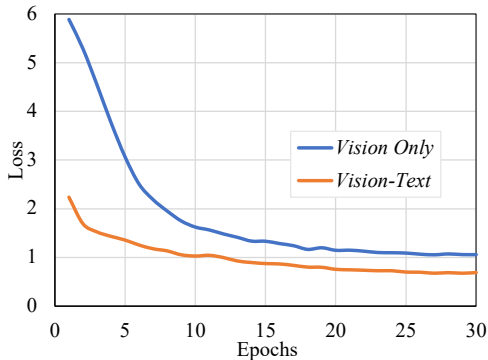
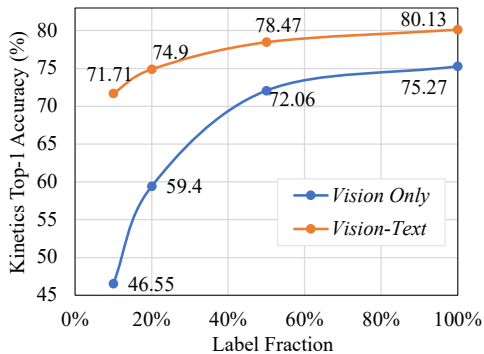


Figure 3: Vision-Text v.s. Vision-only framework under different label fractions on Kinetics-400.

Figure 4: The training loss of Vision-Text and Vision-only framework on Kinetics-400.

**Different assignments to the offline classifier.** We set different initializations described in section 2.2 to the offline classifier  $W \in \mathbb{R}^{d \times c}$  and then train our visual encoder on Kinetics-400. Table 4 lists their comparisons. We show that feeding the offline classifier a random  $d$ -by- $c$  matrix with a normal distribution reduces performance significantly. Then we assign the orthogonal matrix to the classifier, and we can see that having different classes that are orthogonal will result in inferior performance. Also, we choose DistilBERT [65] as the textual encoder to pre-extract the text embeddings of  $c$  categories. The resulting performance is the same as that of the CLIP’s textual encoder. Furthermore, we term the linear discriminate projection as the maximal correlation initialization, as stated in Section 2.2. To do so, we first sample 60 videos from each class in the training set and utilize the pre-trained visual encoder to extract visual embeddings from these 24,000 videos. Finally, we learn the linear classifier by performing linear discriminant analysis on these visual embeddings and their ground-truth labels. We can see that the result of the LDA projection is consistent with our statement. More visualizations of these classifiers are in Appendix §A.3.

Table 4: Exploration of different generation methods for the frozen classifier.

Offline classifier from	Top 1
Textual encoder of CLIP	<b>81.52</b>
Random normal matrix	59.30
Random orthogonal matrix	59.44
DistilBERT	81.45
Linear discriminant projection	80.77

Table 5: Temporal modeling for video encoders.

Backbone	Modeling	Top-1	Top-5
ResNet-50	TAP	71.20	90.37
	T1D	67.18	88.45
	T-Trans	<b>74.26</b>	<b>91.67</b>
ViT-B/16	TAP	80.13	94.98
	TokenT1D	80.42	95.03
	T-Trans	<b>81.52</b>	<b>95.49</b>

**Temporal modeling.** Here we explore more temporal modelings for ViT [33] and ResNet [20]: (1) **TAP**: Temporal average pooling is the most straightforward temporal modeling. (2) **T1D**: The

channel-wise temporal 1D convolutions, is a common strategy [57, 66, 67], to perform efficient temporal interaction in the latter stages (*i.e.*,  $\text{res}_{4-5}$ ) of ResNet. (3) **T-Trans**: The embeddings of frames are fed to a multi-layer (*e.g.*, 6-layer) temporal transformer encoder. (4) **TokenT1D**: We use T1D to model temporal relations for [class] token features that are aggregated from local features via attention in the vision transformer. We perform the TokenT1D in multiple positions of a vision transformer. Results are shown in Table 5. On both backbones, TAP provides simple baselines and T-Trans exhibits the best top-1 accuracy. Both of them maintain the original frame-level representations and then perform temporal modeling. An interesting thing we observed is that T1D does not seem to work in this scenario. The reason lies in that T1D may have the potential to break the learned strong representations provided by CLIP. TokenT1D is another internal-backbone temporal modeling, and it does not yield a performance drop, and even slightly improves the TAP baseline. We believe this is because TokenT1D is only imposed on the global [class] token features instead of patches features, resulting in minimal modifications on pre-trained features.

**Visual encoder with different pre-training.** Besides CLIP-pretrained visual encoders, we further explore our paradigm with different pre-trained visual encoders. As shown in Table 6, equipped with ImageNet-pretrained visual encoder, our method helps to improve the vision-only counterpart by 0.9%. We can see that the CLIP-pretrained visual encoder achieves more significant performance, which is probably because CLIP provides the coarse initial alignment between frames and category names, as well as covers rich visual concepts.

Table 6: Study on different pre-training.

Visual encoder	Paradigm	Top-1
CLIP-pretrained	Vision-Only	75.27
	Vision-Text	<b>80.13</b>
ImageNet-pretrained	Vision-Only	74.78
	Vision-Text	<b>75.63</b>

Table 7: Study on various text input forms.

Text input from	Top 1
class name	81.37
“a video of a person” + class name	<b>81.52</b>
multiple fixed templates + class name	80.88
learnable template + class name	81.22

**Text input forms.** Intuitively, the name of a class appears to be the most straightforward text information. We can see that only using the label text can yield good results in Table 7. Then following the prompt engineering in CLIP [1], we utilize the prompt template “a video of a person {label}.” to help specify the text is about the content of the video. This only slightly increases performance over the baseline of using the label text. We further use multiple prompt templates as the text augmentation during training. Performance decreases by 0.64% on Kinetics-400. This may be because different prompt templates may introduce extra noise for the training. In addition to the hand-crafted prompt, we also adopt an automated prompt [68] to describe a prompt’s context using a set of learnable vectors. The results suggest that different templates have little impact on our model.

Table 8: Different instantiations of our method on Kinetics-400. “Single View” indicates one temporal clip with one spatial crop, whereas “4×3 Views” indicates 4 temporal clips with 3 spatial crops.

Encoder	Resolution	Frames	Single View		4×3 Views	
			Top-1	Top-5	Top-1	Top-5
ResNet-50	224×224	8	74.26	91.67	75.50	92.61
		16	75.50	92.20	76.60	93.12
ViT-B/32	224×224	8	78.54	94.14	80.00	94.84
		16	79.25	94.31	80.51	95.10
ViT-B/16	224×224	8	81.52	95.49	82.90	96.28
		16	82.32	95.90	83.58	96.38
ViT-L/14	224×224	8	85.52	96.72	86.37	97.23
		16	85.94	96.96	86.72	97.28
ViT-L/14	336×336	8	86.33	97.06	87.09	97.38
		16	86.79	97.24	87.56	97.44

**More instantiations.** We assess different instantiations of our paradigm, in terms of different visual encoders, more input frames, and larger spatial resolution. See Appendix §B.2 for more details on architectures. In Table 8, we present the results of our method with two typical evaluation protocols. In general, more frames, larger spatial resolution, and deeper backbones lead to higher accuracy.

Table 9: Ours vs. Matching paradigm with ViT-B/16 on Kinetics-400. The number of V100-days is the number of V100 GPU used for training multiplied by the training time in days. \* indicates the official result [54] via “Data-parallel training” on 3090 GPUs. For efficient training and fair comparison, we implement all experiments with “Distributed Data-parallel training” in the Table.

Method	Batch gather	Textual encoder	Top-1	Top-5	V100-days
Matching paradigm [54]	✓	online	81.15	95.42	6.7 (10*)
	✓	offline	80.73	95.36	6.6
	✗	online	77.77	94.79	3.5
	✗	offline	76.13	94.57	3.3
Our paradigm	✗	offline	<b>81.52</b>	<b>95.49</b>	<b>3.3</b>

**Our recognition paradigm vs. Matching paradigm.** Here we make a comparison with the matching-based method mentioned in Section 3. The matching paradigm treats the recognition task as a video-text matching problem with contrastive loss, thus requiring a batch gathering to collect embeddings of all batches across all GPUs and calculate cosine similarity for a given batch across all other batches. See Appendix §B.3 for details about the batch gathering. In Table 9, we try to compare with the matching paradigm [54] as fairly as we can. We can see that the matching paradigm does not work well without batch gather. This is due to contrastive learning favors a large batch size. Besides, involving batch gather will multiply the training time. Also, in this case, the pre-trained textual encoder still needs to be updated, which requires larger GPU memory. However, our paradigm employs pre-extracted text embeddings as our classifier, so the only thing we need to fine-tune is the visual encoder. Results show that our method achieves the best accuracy-cost trade-off. Specifically, our method achieves the performance of 81.52% with ViT-B/16, which takes only 10 hours to run the training using 8 GPUs (2×faster than the matching counterpart).

## 5 Experiments: Image Recognition

We also evaluate our approach to the image recognition task. Here we conduct experiments on ImageNet [3] and share the same training recipe in section 4.1 with ImageNet.

**Few-shot image recognition.** Here we also use the challenging  $K$ -shot  $C$ -way setting on ImageNet. Specifically, the models are trained using  $K$  images (shots) from the training set for each image category and then measure performance on the corresponding standard 1000-class testing set. As shown in Table 10, the results reveal that our method has strong transferability under data-poor conditions, whereas the standard unimodality paradigm is ineffective in comparison to ours.

Table 10: Few-shot image recognition on ImageNet. “Zero-shot” and “All-shot” denote the lower and upper bounds of the task respectively. Top-1 accuracy is reported here.

K-shot	0	1	3	5	All
Ours	66.73	71.50	73.64	74.99	82.25
Vision-Only	0	4.71	30.44	41.70	79.70

Table 11: Zero-shot image recognition. We train the model on IN600 then perform evaluation on IN400.

IN600→IN400	
Ours w/o train	70.28
Ours w/ train	<b>72.62</b>

**Zero-shot image recognition.** Here we split the ImageNet-1K into two parts, with 600 categories (IN600) for training, and the remaining unseen 400 categories (IN400) for evaluation. Table 11 demonstrates the zero-shot image recognition ability of our method.

**Efficient training.** For readers’ reference, we provide the performance of our approach with different visual backbones on ImageNet in Table 12. Notably, using 8 GPUs, we can train the ViT-B/16 to achieve 82.25% in 90 minutes, while the ViT-L/14 only takes 6 hours to achieve 86.47%.

Table 12: Study on various backbones. Models are trained with 10 epochs.

Backbone	Resolution	Top-1	Top-5	FLOPs	Params	A100-days
VIT-B/16	224×224	83.10	96.94	11.3G	57.3M	0.5
VIT-L/14	224×224	86.72	98.24	51.9G	202.1M	2.0
VIT-L/14	336×336	87.54	98.43	116.5G	202.1M	5.7

## 6 Conclusion

We present a new paradigm for improving the transferability of visual recognition that is based on the knowledge from the textual encoder of the well-trained vision-language model. The empirical study shows that our method improves both the performance and the convergence speed of visual classification. The proposed approach has superior performance on both general and zero-shot/few-shot recognition and achieves state-of-the-art performance on video recognition tasks, and democratizes training on large-scale video/image datasets.

## Appendix

In this appendix, §A contains further *results* for video recognition: the statistics of video datasets (§A.1), comparison with SOTAs on UCF-101 and HMDB-51 (§A.2), more visualizations of different classifier (§A.3) and more ablations (§A.4). §B contains additional *implementation details* for: details of several large-scale datasets for pre-training (§B.1), visual encoder architectures (§B.2), Batch Gather (§B.3) and Text template (§B.4).

### A Additional Results on Video Recognition

#### A.1 Video datasets

- **Kinetics-400** (K400) [12] is a large-scale video dataset, which consists of 240k training videos and 20k validation videos in 400 different human action categories.
- **UCF-101** [13] contains 13k videos spanning over 101 human actions.
- **HMDB-51** [14] contains approximately 7k videos belonging to 51 action class categories.

#### A.2 Comparison with state-of-the-arts on UCF-101 and HMDB-51

We also evaluate our method on the UCF-101 and HMDB-51 datasets to demonstrate its capacity to generalize to smaller datasets. We finetune our models on these two datasets using the pre-trained ViT-L model on Kinetics-400 and present the mean class accuracy over three splits utilizing 8 frames as inputs and 30 epochs for training. Table A.1 reveals that our model has a pretty transfer capability, with mean class accuracy of 98.2% on UCF-101 and 79.0% on HMDB-51, respectively.

Table A.1: **Mean class accuracy** on UCF-101 and HMDB-51 achieved by different methods which are transferred from their **Kinetics** models with RGB modality (over 3 splits).

Method	UCF-101	HMDB-51
ECO <sub>En</sub> [69]	94.8%	72.4%
ARTNet [70]	94.3%	70.9%
I3D [27]	95.6%	74.8%
R(2+1)D [31]	96.8%	74.5%
S3D-G [30]	96.8%	75.9%
TSM [71]	95.9%	73.5%
STM [72]	96.2%	72.2%
TEINet [67]	96.7%	72.1%
MVFNet [57]	96.6%	75.7%
TDN [66]	97.4%	76.4%
Ours	<b>98.2%</b>	<b>79.0%</b>

#### A.3 More visualizations of different classifiers

Here we provide more visualizations of different classifiers in Figure A.5.

#### A.4 Comparison with the unfrozen classifier

As we described in Section 2.2 of the submission, we freeze the classifier from updating during the fine-tuning of the downstream tasks for the reason: It could preserve the textual knowledge from being disturbed by the randomness brought by the mini-batch. By doing so, we can replace the offline classifier and do zero-shot recognition.

Here, we test the unfrozen classifier with the same textual embeddings as the frozen classifier. The unfrozen results are given in Table A.2. We can see that the unfrozen setting causes the original textual knowledge to be broken, resulting in a decrease in performance.

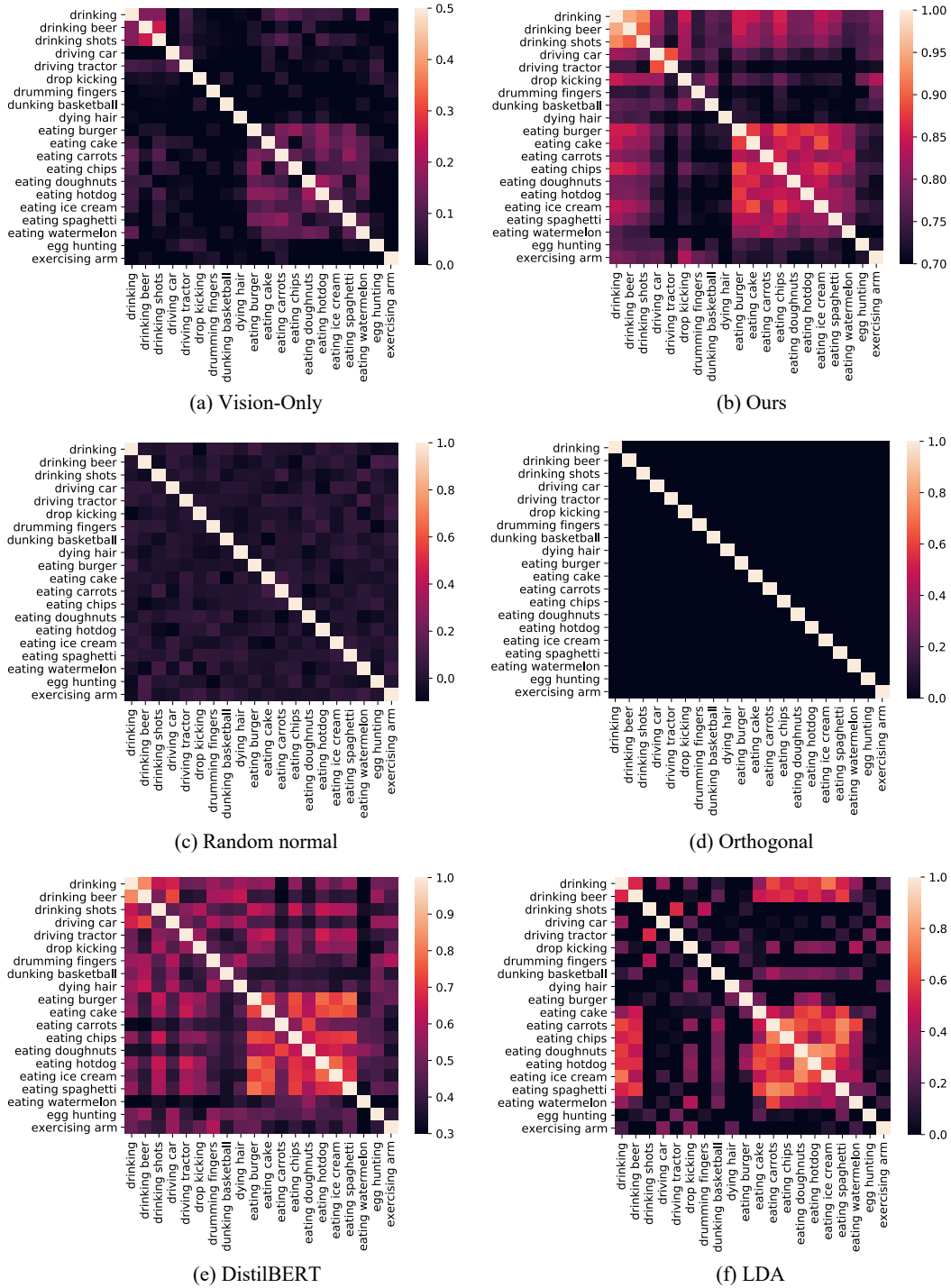


Figure A.5: Inter-class correlation maps of “embeddings of class labels” for 20 categories on Kinetics-400. The color thresholds are adjusted for better understandability. Please zoom in for best view.

Table A.2: Frozen classifier vs. Unfrozen classifier.

Setting	Top-1	Top-5
frozen	81.52	95.49
unfrozen	79.16	93.55

## B Additional Implementation Details

### B.1 Large-scale datasets for pre-training

Here we describe the large-scale web-scale datasets used in other video recognition methods for pre-training. The suffix of the name represents the magnitude of the dataset.

- **ImageNet-1K/21K**: The ImageNet-1K dataset was used to pre-train models for computer vision transfer learning. It was first released for the ILSVRC2012 visual recognition challenge. The ImageNet-1K dataset is a subset of the larger ImageNet dataset, which contains 14,197,122 images split into 21,841 categories. The whole dataset is known to as ImageNet-21K (sometimes referred to as ImageNet-22K) and has been **open-source**<sup>3</sup>. ImageNet-1K was created by selecting a subset of 1.2M images from ImageNet-21K, that belong to 1000 mutually exclusive classes.
- **IG-65M**: Facebook has proposed the IG-65M dataset, which contains approximately 65 million public, user-generated Instagram videos with hashtags. Due to label and temporal noise, the dataset is used for weakly-supervised training. This dataset is not open-source, but several pre-trained R(2+1)D [31] and CSN [59] models are **provided**<sup>4</sup>.
- **JFT-300M**: JFT-300M is an internal Google dataset used to train image classification models. The dataset consists of 300M images that are labeled with 18,291 categories. Image labels are generated using a complex algorithm that combines raw web signals, web page connections, and user feedback. However, the dataset and the pre-trained weights are **not** open-source.
- **FLD-900M**: FLD-900M is a large image-caption dataset from Microsoft, which includes 900M Images and 900M Free form text (From one word, Phrase to sentence). By now, the dataset and the pre-trained weights are **not** open-source.
- **JFT-3B**: JFT-3B is an internal Google dataset and a larger version of the JFT-300M. It has over 3 billion images that have been annotated with a class structure of around 30k labels using a semi-automated procedure. Also, the dataset and the pre-trained weights are **not** open-source.
- **WIT-400M**: WIT-400M is a dataset that contains 400 million web image-text pairs, and is used to train CLIP [1]. CLIP does not release the dataset, but made all of the pre-trained models **available**<sup>5</sup>. In this paper, we utilize the CLIP-pretrained models in our experiments.

### B.2 Visual encoder architectures

In this paper, we use the visual encoder and textual encoder as shown in Table A.3 and A.4.

Table A.3: CLIP-ResNet hyperparameters

Model	Embedding dimension	Input resolution	ResNet		Text Transformer		
			blocks	width	layers	width	heads
RN50	1024	224	(3, 4, 6, 3)	2048	12	512	8

<sup>3</sup><https://www.image-net.org>

<sup>4</sup><https://github.com/facebookresearch/vmz>

<sup>5</sup><https://github.com/openai/CLIP>

Table A.4: CLIP-ViT hyperparameters

Model	Embedding dimension	Input resolution	Vision Transformer			Text Transformer		
			layers	width	heads	layers	width	heads
ViT-B/32	512	224	12	768	12	12	512	8
ViT-B/16	512	224	12	768	12	12	512	8
ViT-L/14	768	224	24	1024	16	12	768	12
ViT-L/14-336px	768	336	24	1024	16	12	768	12

### B.3 Batch Gather for Distributed InfoNCE

Instead of Data-Parallel Training (DP), which is single-process, multi-thread, and only works on a single machine, Distributed Data-Parallel Training (DDP) is a widely adopted single-program multiple-data training paradigm for single- and multi-machine training. Due to GIL contention across threads, per-iteration replicated model, and additional overhead introduced by scattering inputs and gathering outputs, DP is usually slower than DDP even on a single machine.

---

**Algorithm 1:** Numpy-like Pseudocode that illustrates the role of Batch Gather in Distributed InfoNCE.

---

```

# text_encoder: encoder network for text input
# vision_encoder: encoder network for vision input, e.g., images or videos.
# V: minibatch of vision inputs
# T: minibatch of text inputs
# N: the local batch size of each GPU, e.g.,16
# M: the number of GPUs, e.g.,8
# N * M: the global batch size for multi-gpu training, e.g.,128

# extract feature representations of each modality
local_vision_features = vision_encoder(V) # shape: [N, embed_dim]
local_text_features = text_encoder(T) # shape: [N, embed_dim]

# normalization
local_vision_features = l2_normalize(local_vision_features, axis=1)
local_text_features = l2_normalize(local_text_features, axis=1)

# batch_gather is a function gathering and concatenating the tensors across GPUs.
all_vision_features = batch_gather(local_vision_features) # shape: [N * M, embed_dim]
all_text_features = batch_gather(local_text_features) # shape: [N * M, embed_dim]

# scaled pairwise cosine similarities
# shape = [N, N * M]
logits_per_image = logit_scale * image_features @ all_text_features.t()
# shape = [N, N * M]
logits_per_text = logit_scale * text_features @ all_image_features.t()

# The logits are then used as inputs for N*M-way (e.g., 128-way) classification,
# resulting in a loss value corresponding to N inputs in each GPU.
# Then Distributed Data Parallel mechanism takes care of averaging these across GPUs,
# which becomes equivalent to calculating the loss over NMxNM (e.g.,128x128) similarities.

```

---

Hence, we develop the Distributed InfoNCE based on DDP for large batch size and fast training. The core of the Distributed InfoNCE implementation is batch gathering. Say there are  $M$  GPUs and each GPU gets  $N$  input pairs, we need to calculate the  $NM \times NM$  similarity matrix across the GPUs for InfoNCE loss. Without batch gathering, each GPU only computes a local  $N \times N$  matrix, *s.t.*  $N \ll NM$ . Then the cosine similarity and the InfoNCE loss would be calculated only for the pairs within a single GPU and later their gradients would be averaged and synced. That’s obviously not what we want.

The batch gathering for Distributed InfoNCE is presented as follows. When calculating the similarity matrix (and thus the logit scores across text inputs for each image/video), a GPU only needs to hold  $M$  vision features, and perform matrix product with  $NM$  text features, yielding an  $M \times NM$  matrix. This computation is distributed (*i.e.*, sharded) across  $N$  GPUs, and we have calculated  $NM \times NM$  similarities across the GPUs in total. The loss we employ is symmetric and the same happens *w.r.t.*

text inputs. As shown in Algorithm 1, we also give an example pseudocode to help you understand the statement.

#### B.4 Text template

In Table 4 of the submission, we study several text input forms, including class names, single hard template, multiple hard templates, and learnable templates. More details are as follows:

**Class name** To build textual embeddings, we utilize the category names of the dataset as the text input, e.g., “*eating hotdog*”, “*driving car*”, etc.

**Single hard template** We employ the hand-crafted template “*a video of a person {class name}.*” to form a sentence as input.

**Multiple hard templates** CLIP<sup>6</sup> provides 28 templates for Kinetics, one of which is the above single template. We use these multiple templates as the text augmentation during training. At each iteration, we choose one template at random as text input. Then, using the above single hard template as input, we perform the evaluation.

**Learnable templates** We adopt the automated prompt CoOp [68] to describe a prompt’s context using a set of learnable vectors. Specifically, the prompt given to the text encoder is designed with the following form,

$$t = [V]_1[V]_2 \dots [V]_M[\text{class name}], \quad (7)$$

where each  $[V]_m$  ( $m \in \{1, \dots, M\}$ ) is a vector of the same size as word embeddings, and  $M$  is a hyperparameter indicating the number of context tokens. We set the  $M$  to 4.

---

<sup>6</sup><https://github.com/openai/CLIP/blob/main/data/prompts.md>

## References

- [1] Alec Radford, Jong Wook Kim, Chris Hallacy, Aditya Ramesh, Gabriel Goh, Sandhini Agarwal, Girish Sastry, Amanda Askell, Pamela Mishkin, Jack Clark, et al. Learning transferable visual models from natural language supervision. In *International Conference on Machine Learning*, pages 8748–8763. PMLR, 2021.
- [2] Chen Sun, Abhinav Shrivastava, Saurabh Singh, and Abhinav Gupta. Revisiting unreasonable effectiveness of data in deep learning era. In *Proceedings of the IEEE international conference on computer vision*, pages 843–852, 2017.
- [3] Jia Deng, Wei Dong, Richard Socher, Li-Jia Li, Kai Li, and Li Fei-Fei. Imagenet: A large-scale hierarchical image database. In *Proc. CVPR*, 2009.
- [4] Tal Ridnik, Emanuel Ben-Baruch, Asaf Noy, and Lihi Zelnik-Manor. Imagenet-21k pretraining for the masses. *arXiv preprint arXiv:2104.10972*, 2021.
- [5] Xiaohua Zhai, Alexander Kolesnikov, Neil Houlsby, and Lucas Beyer. Scaling vision transformers. In *arXiv preprint arXiv:2106.04560*, 2021.
- [6] Chao Jia, Yinfei Yang, Ye Xia, Yi-Ting Chen, Zarana Parekh, Hieu Pham, Quoc Le, Yun-Hsuan Sung, Zhen Li, and Tom Duerig. Scaling up visual and vision-language representation learning with noisy text supervision. In *International Conference on Machine Learning*, pages 4904–4916. PMLR, 2021.
- [7] Priya Goyal, Mathilde Caron, Benjamin Lefaudeaux, Min Xu, Pengchao Wang, Vivek Pai, Manat Singh, Vitaliy Liptchinsky, Ishan Misra, Armand Joulin, et al. Self-supervised pretraining of visual features in the wild. *arXiv preprint arXiv:2103.01988*, 2021.
- [8] Kaiming He, Haoqi Fan, Yuxin Wu, Saining Xie, and Ross Girshick. Momentum contrast for unsupervised visual representation learning. In *Proceedings of the IEEE/CVF conference on computer vision and pattern recognition*, pages 9729–9738, 2020.
- [9] Ron Mokady, Amir Hertz, and Amit H Bermano. Clipcap: Clip prefix for image captioning. *arXiv preprint arXiv:2111.09734*, 2021.
- [10] Aditya Ramesh, Mikhail Pavlov, Gabriel Goh, Scott Gray, Chelsea Voss, Alec Radford, Mark Chen, and Ilya Sutskever. Zero-shot text-to-image generation. In *International Conference on Machine Learning*, pages 8821–8831. PMLR, 2021.
- [11] Aditya Ramesh, Prafulla Dhariwal, Alex Nichol, Casey Chu, and Mark Chen. Hierarchical text-conditional image generation with clip latents. *arXiv preprint arXiv:2204.06125*, 2022.
- [12] Will Kay, Joao Carreira, Karen Simonyan, Brian Zhang, Chloe Hillier, Sudheendra Vijayanarasimhan, Fabio Viola, Tim Green, Trevor Back, Paul Natsev, et al. The kinetics human action video dataset. *arXiv preprint arXiv:1705.06950*, 2017.
- [13] Khurram Soomro, Amir Roshan Zamir, and Mubarak Shah. Ucf101: A dataset of 101 human actions classes from videos in the wild. *arXiv preprint arXiv:1212.0402*, 2012.
- [14] Hildegard Kuehne, Hueihan Jhuang, Estíbaliz Garrote, Tomaso Poggio, and Thomas Serre. Hmdb: a large video database for human motion recognition. In *Proc. ICCV*, 2011.
- [15] Aaron Van den Oord, Yazhe Li, and Oriol Vinyals. Representation learning with contrastive predictive coding. *arXiv e-prints*, pages arXiv–1807, 2018.
- [16] Cheng-I Lai. Contrastive predictive coding based feature for automatic speaker verification. *arXiv preprint arXiv:1904.01575*, 2019.
- [17] Xinlei Chen, Saining Xie, and Kaiming He. An empirical study of training self-supervised vision transformers. In *Proceedings of the IEEE/CVF International Conference on Computer Vision*, pages 9640–9649, 2021.
- [18] Tao Li, Shenghuo Zhu, and Mitsunori Ogihara. Using discriminant analysis for multi-class classification: an experimental investigation. *Knowledge and information systems*, 10(4):453–472, 2006.
- [19] Alex Krizhevsky, Ilya Sutskever, and Geoffrey E Hinton. Imagenet classification with deep convolutional neural networks. *Advances in neural information processing systems*, 25, 2012.
- [20] Kaiming He, Xiangyu Zhang, Shaoqing Ren, and Jian Sun. Deep residual learning for image recognition. In *Proc. CVPR*, 2016.

- [21] Karen Simonyan and Andrew Zisserman. Very deep convolutional networks for large-scale image recognition. *arXiv preprint arXiv:1409.1556*, 2014.
- [22] Yemin Shi, Yonghong Tian, Yaowei Wang, Wei Zeng, and Tiejun Huang. Learning long-term dependencies for action recognition with a biologically-inspired deep network. In *Proc. ICCV*, 2017.
- [23] Andrew G Howard, Menglong Zhu, Bo Chen, Dmitry Kalenichenko, Weijun Wang, Tobias Weyand, Marco Andreetto, and Hartwig Adam. Mobilenets: Efficient convolutional neural networks for mobile vision applications. *arXiv preprint arXiv:1704.04861*, 2017.
- [24] Mingxing Tan and Quoc Le. Efficientnet: Rethinking model scaling for convolutional neural networks. In *International conference on machine learning*, pages 6105–6114. PMLR, 2019.
- [25] Karen Simonyan and Andrew Zisserman. Two-stream convolutional networks for action recognition in videos. In *Neurips*, 2014.
- [26] Limin Wang, Yuanjun Xiong, Zhe Wang, Yu Qiao, Dahua Lin, Xiaoou Tang, and Luc Van Gool. Temporal segment networks: Towards good practices for deep action recognition. In *Proc. ECCV*, 2016.
- [27] Joao Carreira and Andrew Zisserman. Quo vadis, action recognition? a new model and the kinetics dataset. In *Proc. CVPR*, 2017.
- [28] Du Tran, Lubomir Bourdev, Rob Fergus, Lorenzo Torresani, and Manohar Paluri. Learning spatiotemporal features with 3d convolutional networks. In *Proc. ICCV*, 2015.
- [29] Zhaofan Qiu, Ting Yao, and Tao Mei. Learning spatio-temporal representation with pseudo-3d residual networks. In *Proc. ICCV*, 2017.
- [30] Saining Xie, Chen Sun, Jonathan Huang, Zhuowen Tu, and Kevin Murphy. Rethinking spatiotemporal feature learning: Speed-accuracy trade-offs in video classification. In *Proc. ECCV*, 2018.
- [31] Du Tran, Heng Wang, Lorenzo Torresani, Jamie Ray, Yann LeCun, and Manohar Paluri. A closer look at spatiotemporal convolutions for action recognition. In *Proc. CVPR*, 2018.
- [32] Ashish Vaswani, Noam Shazeer, Niki Parmar, Jakob Uszkoreit, Llion Jones, Aidan N Gomez, Łukasz Kaiser, and Illia Polosukhin. Attention is all you need. In *Advances in neural information processing systems*, pages 5998–6008, 2017.
- [33] Alexey Dosovitskiy, Lucas Beyer, Alexander Kolesnikov, Dirk Weissenborn, Xiaohua Zhai, Thomas Unterthiner, Mostafa Dehghani, Matthias Minderer, Georg Heigold, Sylvain Gelly, et al. An image is worth 16x16 words: Transformers for image recognition at scale. *arXiv preprint arXiv:2010.11929*, 2020.
- [34] Kai Han, An Xiao, Enhua Wu, Jianyuan Guo, Chunjing Xu, and Yunhe Wang. Transformer in transformer. *Advances in Neural Information Processing Systems*, 34, 2021.
- [35] Ze Liu, Yutong Lin, Yue Cao, Han Hu, Yixuan Wei, Zheng Zhang, Stephen Lin, and Baining Guo. Swin transformer: Hierarchical vision transformer using shifted windows. In *Proceedings of the IEEE/CVF International Conference on Computer Vision*, pages 10012–10022, 2021.
- [36] Gedas Bertasius, Heng Wang, and Lorenzo Torresani. Is space-time attention all you need for video understanding? In *ICML*, pages 813–824. PMLR, 2021.
- [37] Anurag Arnab, Mostafa Dehghani, Georg Heigold, Chen Sun, Mario Lučić, and Cordelia Schmid. Vivit: A video vision transformer. *Proc. ICCV*, 2021.
- [38] Ze Liu, Jia Ning, Yue Cao, Yixuan Wei, Zheng Zhang, Stephen Lin, and Han Hu. Video swin transformer. *arXiv preprint arXiv:2106.13230*, 2021.
- [39] Haoqi Fan, Bo Xiong, Karttikeya Mangalam, Yanghao Li, Zhicheng Yan, Jitendra Malik, and Christoph Feichtenhofer. Multiscale vision transformers. *Proc. ICCV*, 2021.
- [40] Aaron Van den Oord, Yazhe Li, and Oriol Vinyals. Representation learning with contrastive predictive coding. *arXiv e-prints*, pages arXiv–1807, 2018.
- [41] Chao Jia, Yinfei Yang, Ye Xia, Yi-Ting Chen, Zarana Parekh, Hieu Pham, Quoc Le, Yun-Hsuan Sung, Zhen Li, and Tom Duerig. Scaling up visual and vision-language representation learning with noisy text supervision. In *International Conference on Machine Learning*, pages 4904–4916. PMLR, 2021.

- [42] Junnan Li, Dongxu Li, Caiming Xiong, and Steven Hoi. Blip: Bootstrapping language-image pre-training for unified vision-language understanding and generation. *arXiv preprint arXiv:2201.12086*, 2022.
- [43] Yangguang Li, Feng Liang, Lichen Zhao, Yufeng Cui, Wanli Ouyang, Jing Shao, Fengwei Yu, and Junjie Yan. Supervision exists everywhere: A data efficient contrastive language-image pre-training paradigm. *arXiv preprint arXiv:2110.05208*, 2021.
- [44] Lu Yuan, Dongdong Chen, Yi-Ling Chen, Noel Codella, Xiyang Dai, Jianfeng Gao, Houdong Hu, Xuedong Huang, Boxin Li, Chunyuan Li, et al. Florence: A new foundation model for computer vision. *arXiv preprint arXiv:2111.11432*, 2021.
- [45] Jiahui Yu, Zirui Wang, Vijay Vasudevan, Legg Yeung, Mojtaba Seyedhosseini, and Yonghui Wu. Coca: Contrastive captioners are image-text foundation models. *arXiv preprint arXiv:2205.01917*, 2022.
- [46] Jianwei Yang, Chunyuan Li, Pengchuan Zhang, Bin Xiao, Ce Liu, Lu Yuan, and Jianfeng Gao. Unified contrastive learning in image-text-label space. *arXiv preprint arXiv:2204.03610*, 2022.
- [47] Antoine Miech, Jean-Baptiste Alayrac, Lucas Smaira, Ivan Laptev, Josef Sivic, and Andrew Zisserman. End-to-end learning of visual representations from uncurated instructional videos. In *Proceedings of the IEEE/CVF Conference on Computer Vision and Pattern Recognition*, pages 9879–9889, 2020.
- [48] Max Bain, Arsha Nagrani, Gül Varol, and Andrew Zisserman. Frozen in time: A joint video and image encoder for end-to-end retrieval. In *Proceedings of the IEEE/CVF International Conference on Computer Vision*, pages 1728–1738, 2021.
- [49] Huaishao Luo, Lei Ji, Ming Zhong, Yang Chen, Wen Lei, Nan Duan, and Tianrui Li. Clip4clip: An empirical study of clip for end to end video clip retrieval. *arXiv preprint arXiv:2104.08860*, 2021.
- [50] Linchao Zhu and Yi Yang. Actbert: Learning global-local video-text representations. In *Proceedings of the IEEE/CVF conference on computer vision and pattern recognition*, pages 8746–8755, 2020.
- [51] Xiaohan Wang, Linchao Zhu, and Yi Yang. T2vlad: global-local sequence alignment for text-video retrieval. In *Proceedings of the IEEE/CVF Conference on Computer Vision and Pattern Recognition*, pages 5079–5088, 2021.
- [52] Shuai Zhao, Linchao Zhu, Xiaohan Wang, and Yi Yang. Centerclip: Token clustering for efficient text-video retrieval. *The 45th International ACM SIGIR Conference on Research and Development in Information Retrieval*, 2022.
- [53] Jie Lei, Linjie Li, Luwei Zhou, Zhe Gan, Tamara L Berg, Mohit Bansal, and Jingjing Liu. Less is more: Clipbert for video-and-language learning via sparse sampling. In *Proceedings of the IEEE/CVF Conference on Computer Vision and Pattern Recognition*, pages 7331–7341, 2021.
- [54] Mengmeng Wang, Jiazheng Xing, and Yong Liu. Actionclip: A new paradigm for video action recognition. *arXiv preprint arXiv:2109.08472*, 2021.
- [55] Chen Ju, Tengda Han, Kunhao Zheng, Ya Zhang, and Weidi Xie. Prompting visual-language models for efficient video understanding. *arXiv preprint arXiv:2112.04478*, 2021.
- [56] Christoph Feichtenhofer, Haoqi Fan, Jitendra Malik, and Kaiming He. Slowfast networks for video recognition. *Proc. ICCV*, 2019.
- [57] Wenhao Wu, Dongliang He, Tianwei Lin, Fu Li, Chuang Gan, and Errui Ding. Mvfnnet: Multi-view fusion network for efficient video recognition. In *Proc. AAAI*, 2021.
- [58] Christoph Feichtenhofer. X3d: Expanding architectures for efficient video recognition. In *Proc. CVPR*, pages 203–213, 2020.
- [59] Du Tran, Heng Wang, Lorenzo Torresani, and Matt Feiszli. Video classification with channel-separated convolutional networks. In *Proc. ICCV*, pages 5552–5561, 2019.
- [60] Michael S Ryoo, AJ Piergiovanni, Anurag Arnab, Mostafa Dehghani, and Anelia Angelova. Tokenlearner: What can 8 learned tokens do for images and videos? *arXiv preprint arXiv:2106.11297*, 2021.
- [61] Shen Yan, Xuehan Xiong, Anurag Arnab, Zhichao Lu, Mi Zhang, Chen Sun, and Cordelia Schmid. Multiview transformers for video recognition. *arXiv preprint arXiv:2201.04288*, 2022.

- [62] Bowen Zhang, Jiahui Yu, Christopher Fifty, Wei Han, Andrew M Dai, Ruoming Pang, and Fei Sha. Co-training transformer with videos and images improves action recognition. *arXiv preprint arXiv:2112.07175*, 2021.
- [63] Deepti Ghadiyaram, Du Tran, and Dhruv Mahajan. Large-scale weakly-supervised pre-training for video action recognition. In *Proceedings of the IEEE/CVF conference on computer vision and pattern recognition*, pages 12046–12055, 2019.
- [64] Michael McCloskey and Neal J Cohen. Catastrophic interference in connectionist networks: The sequential learning problem. In *Psychology of learning and motivation*, volume 24, pages 109–165. Elsevier, 1989.
- [65] Victor Sanh, Lysandre Debut, Julien Chaumond, and Thomas Wolf. Distilbert, a distilled version of bert: smaller, faster, cheaper and lighter. *arXiv preprint arXiv:1910.01108*, 2019.
- [66] Limin Wang, Zhan Tong, Bin Ji, and Gangshan Wu. Tdn: Temporal difference networks for efficient action recognition. In *Proceedings of the IEEE/CVF Conference on Computer Vision and Pattern Recognition*, pages 1895–1904, 2021.
- [67] Zhaoyang Liu, Donghao Luo, Yabiao Wang, Limin Wang, Ying Tai, Chengjie Wang, Jilin Li, Feiyue Huang, and Tong Lu. Teinet: Towards an efficient architecture for video recognition. In *Proc. AAAI*, pages 11669–11676, 2020.
- [68] Kaiyang Zhou, Jingkang Yang, Chen Change Loy, and Ziwei Liu. Learning to prompt for vision-language models. *arXiv preprint arXiv:2109.01134*, 2021.
- [69] Mohammadreza Zolfaghari, Kamaljeet Singh, and Thomas Brox. Eco: Efficient convolutional network for online video understanding. In *Proc. ECCV*, 2018.
- [70] Limin Wang, Wei Li, Wen Li, and Luc Van Gool. Appearance-and-relation networks for video classification. In *Proc. CVPR*, 2018.
- [71] Ji Lin, Chuang Gan, and Song Han. Tsm: Temporal shift module for efficient video understanding. In *Proc. ICCV*, 2019.
- [72] Boyuan Jiang, MengMeng Wang, Weihao Gan, Wei Wu, and Junjie Yan. Stm: Spatiotemporal and motion encoding for action recognition. In *Proc. ICCV*, pages 2000–2009, 2019.